European Rotorcraft Forum

AN ENERGY-BASED TRIM PROCEDURE FOR MULTIROTOR VTOLS

Giovanni Bernardini, giovanni.bernardini@uniroma3.it, Roma Tre University (Italy)
Federico Porcacchia, federico.porcacchia@leonardocompany.com, Leonardo Helicopters (Italy)
Caterina Poggi, caterina.poggi@uniroma3.it, Roma Tre University (Italy)
Massimo Gennaretti, massimo.gennaretti@uniroma3.it, Roma Tre University (Italy)

Abstract
The aim of the proposed paper is the development of a general approach capable of determining the set of trim commands, aerodynamic controls surfaces actuation and/or engine thrust regulation, that allow specific steady-state flight conditions of non-conventional VTOLs, under given performance constraints. Specifically, an energy-based trim algorithm is introduced, based on the minimisation of a cost function. This approach is particularly interesting in that, in case of multi-rotor system, it allows to determine the control settings such to guarantee the required flight condition while using the redundant controls to optimise selected target functions, as for instance performance or noise emission. The proposed approach will be applied to a quadcopter configuration, for validation purposes, and a hexacopter configuration for which a comparison with a conventional trim procedure will be performed. Three different control strategies are applied: a pure rotor angular velocity control, a pure blade collective pitch control and a combined angular velocity and blade collective pitch control.

1. INTRODUCTION

Due to the exponential growth of urban overcrowding and pollution, the identification of alternative and environmentally sustainable solutions to the city traffic is nowadays a crucial issue. This has led to an ever-growing interest towards Urban Air Mobility (UAM) systems, which represent a potential answer to the infrastructure congestion, overcoming the limited capacity of ground transport. Indeed, evolving the mobility from two to three dimensions by introducing fully-electric vertical takeoff and landing (eVTOL) vehicles, represents not only a faster and reliable mode of transportation, but also an energy-efficient, safer, and quieter solution [1]. The development of electrical machinery and the availability of reliable avionic components and composite materials have made the UAM aviation a possible scenario, [2] and great effort is being made nowadays for the development and manufacturing of environmentally sustainable eVTOL prototypes. [3]

In this framework, the development of flight vehicles with capabilities to reach efficiently fast cruise velocities to cover city-city or city-airports civilian air routes and to have access to vertiports and landing pads within the city landscape, is leading to the design of various and unconventional VTOLs configurations [4, 5, 6]. These include different combinations of tilting rotors and fixed wings, with the double purpose of generating lift and aerodynamic control loads. Although, in principle, the availability of more sources of lift and aerodynamic controls represents an unquestionable advantage in terms of controllability, safety, and versatility, unavoidably, it raises the question of which is their most efficient/effective combination to guarantee specific trimmed flight conditions.

In the case of conventional aeronautical vehicles, such as airplanes and helicopters, four commands ensure the trimmed flight providing a unique feasible set of forces and moments capable of governing flight trajectory, attitude and rates. Conversely, for configurations such as multi-rotor aircraft, tiltrotors and compound vehicles, the relationship between the available commands and generated control forces and moments is not bijective. Indeed, depending on the position in the flight envelope, these aircraft can be controlled by different sets of controls, each producing a suitable set of trimming

Copyright Statement
The authors confirm that they, and/or their company or organization, hold copyright on all of the original material included in this paper. The authors also confirm that they have obtained permission, from the copyright holder of any third party material included in this paper, to publish it as part of their paper. The authors confirm that they give permission, or have obtained permission from the copyright holder of this paper, for the publication and distribution of this paper as part of the ERF proceedings or as individual offprints from the proceedings and for inclusion in a freely accessible web-based repository.

forces and moments (see, for instance, the several combinations of elevator and the cyclic longitudinal proprotor control that might be equivalently applied for the trim of a tiltrotor for a wide range of advancing velocities and nacelle orientation). Sets of equivalent controls may provide the same given trim (trajectory, velocity) operating condition, with different attitudes and aerodynamic performance. Thus the capability to select the most suitable set of commands can be of crucial importance under many aspects, such as: i) the definition of optimal conversion corridors of tilting rotor configurations; ii) the definition of the best vehicle performance operating condition; iii) the identification of the load pattern corresponding to reduced structural loads; iv) the definition of the optimal operating condition in terms of minimum acoustic nuisance [7]. To the authors' knowledge, currently, these issues are only partially considered in the vehicle trim process through empirical approaches, rather than by a structured approach as that achievable through the methodology herein proposed.

In recent years many approaches to trim multirotor systems with redundant controls were proposed. Among them the Moore-Penrose pseudo inverse matrix method solves a system of equations with the number of unknowns greater than the number of equations [8]. It provides a not unique set of unknowns that satisfies the trimmed flight equations. Alternatively, the multirotor transformation [9], which is strictly related to the Coleman transformation [10], transforms each rotor's collective pitch and/or angular rotor velocity in a set of equivalent vehicle global controls. The elimination of eventual further redundant controls yields the algebraic problem closure in terms of a suitable set of unknowns (collective, cyclic and differential controls). Then, the inverse multirotor transformation gives the controls of each rotor. Note that, these two approaches are typically unsuitable for the definition of models intended for other design purposes.

The methodology herein proposed overcomes this limitation by recasting the trim problem into an energy function minimization problem which provides the optimal combination of controls that guarantees steady-state flight conditions and the achievement of targeted design objectives. For instance, it can be suitably used to determine the trimmed configuration which corresponds to the minimum control energy or to the optimal aerodynamic performance or to the minimum noise emissions [11].

In this work, the effectiveness of the proposed energy-based method is assessed and compared with that of the aforementioned conventional approaches. Three different trim strategies are analysed: i) rotor angular velocity command, ii) blade collective pitch command, iii) combined angular velocity and blade collective pitch commands. Furthermore, the computational efficiency of the algorithm used to apply the proposed methodology is investigated. Specifically, the Newton-Raphson algorithm and the Sequential Quadratic Programming (SLSQP) are examined, in combination with the multirotor-transformation introduced to reduce the number of the unknowns.

The paper is structured as follows: first, in Sec. 2 the proposed energy-based trim algorithm and the numerical strategies adopted to solve it are outlined and discussed in detail. Then in Sec. 3 the results of an extensive numerical investigation are shown to demonstrate its capability to provide different effective trim strategies for multirotor configurations (in particular, quadcopter and hexacopter VTOLs). Finally, Sec. 4 outlines the main outocomes of the proposed investigations.

2. PROBLEM STATEMENT

The determination of aircraft steady-state flight conditions (i.e., steady level/descent/climb flights and coordinated turns), also called trimmed states, requires the generation of aerodynamic forces on the control surfaces such to assure balance of forces and moments, for a suitable aircraft attitude. The definition of these control actions derives from the solution of the following system of equations[12, 10]

$$
\begin{cases}
X - mg\sin\theta = m\left(qw - rv\right) \\
Y + mg\cos\theta\sin\phi = m\left(ru - pw\right) \\
Z + mg\cos\theta\cos\phi = m\left(pv - qu\right) \\
L = qr\left(I_z - I_y\right) - I_{zx}pq \\
M = rp\left(I_z - I_x\right) + I_{zx}\left(p^2 - r^2\right) \\
N = pq\left(I_y - I_x\right) + I_{zx}qr \\
p = -\dot{\psi}\sin\theta \\
q = \dot{\psi}\cos\theta\sin\phi \\
r = \dot{\psi}\cos\theta\cos\phi
\end{cases}
\tag{1}
$$

where X, Y, Z, L, M, N denote the aerodynamic and propulsive forces and moments applied to the body, m is the vehicle mass, whereas I_x, I_y, I_z and I_{zx} denote inertial moments and product of inertia, respectively. Furthermore, considering the center of mass velocity and the airframe

angular velocity with respect to the ground, u, v, w, p, q, r represent their components in a reference frame rigidly connected with the body, whereas ψ, θ and ϕ are the Euler's angles that define the body orientation with respect to the inertial frame. Note that, the first six equations in Eq. (1) are the aircraft equilibrium equations (linear and angular momentum), while the last three are a set of auxiliary kinematic equations relating the Euler's angles with the components of the body angular velocity. Inertial and kinematic contributions to these equations are nonlinear, with further nonlinear terms deriving from the aerodynamic loads, which are nonlinear functions of the body linear and angular velocity.

Let us indicate with $\mathbf{u}$ the n-dimensional vector of the flight commands, u_i. Then, denoting with $\mathbf{x}$ the aircraft flight state parameters (i.e., $u, v, w, p, q, r, \theta, \phi, \psi$), the set of 9 nonlinear algebraic equations with $9+n$ unknowns expressed in Eq. (1) can be rewritten in compact form as $\mathbf{f}(\mathbf{x}, \mathbf{u}) = \mathbf{0}$. Usually, the number of unknowns reduces to $5+n$ (namely, $p, q, r, \theta, \phi, u_i$) by imposing the four parameters through which a specific steady flight condition is defined.

If the number of commands is $n = 4$, the problem is algebraically well-posed and an acceptable solution, $(\mathbf{x}, \mathbf{u})$, can be straightforwardly obtained by an iterative root finding procedure as the Newton-Raphson or semi-Newton methods or, the bisection methods. [13]

Instead, if $n \neq 4$ the solution of the system $\mathbf{f}(\mathbf{x}, \mathbf{u}) = \mathbf{0}$ can be searched by application of the Newton-Raphson method combined with the introduction of the Moore–Penrose pseudo-inversion: for $n < 4$ the solution is determined as that providing the least mean square error and the condition $\mathbf{f}(\mathbf{x}, \mathbf{u}) = \mathbf{0}$ is not exactly satisfied, whereas for $n > 4$ an infinite number of exact solutions can be derived[8] (note that alternatively, in this latter case, an exact solution can be determined by imposing a suitable number of constraints among the commands).

The case $n > 4$ is typical for the non-conventional multi-rotor architectures, for which a redundant set of commands is usually present. The outline of a methodology aimed at defining the optimal combination of commands trimming the rotorcraft is the objective of this paper.

2.1. Energy-based trim procedure

Different strategies are already available in the literature for the trim analysis of multi-rotor systems, with the most commonly applied that use the pseudo-inverse method [8] and the multi-rotor coordinate transform [9]. However, both these strategies have non-negligible drawbacks. The first approach presents a solution that strongly depends on the starting point of the iterative root-finding procedure and requires an appropriate definition of the bounds of the unknowns in order to avoid non-physical solutions. Instead, the main limitation of the second approach is that it can be applied to multirotor configurations only, in that it is unable for applications to control surfaces like flaps or ailerons.

Here, with the aim of defining a more general approach capable of dealing with multirotor configurations including compound aircraft (like the tiltrotor), it is proposed to recast the trim problem into a minimum energy problem.

Specifically, once defined the energy function, $E(\mathbf{x}, \mathbf{u})$, to be minimized, its minimum is searched under the constraint to comply with the steady-state flight mechanics equations in Eq. 1. This implies the introduction of the Lagrange multipliers, $\boldsymbol{\lambda}$, and the transformation of the original minimum-energy problem into the following one [14]

$$F(\mathbf{x}, \mathbf{u}, \boldsymbol{\lambda}) = E(\mathbf{x}, \mathbf{u}) + \boldsymbol{\lambda}^{\mathsf{T}} \mathbf{f}(\mathbf{x}, \mathbf{u}) = \mathbf{min} \tag{2}$$

Note that the designer can arbitrarily define the energy function in terms of suitable measures of targeted performance (e.g., fuel consumption, noise, etc.), as long as they depend on any of the flight variables and the flight parameters involved in the problem. Note also that, in the corresponding nonlinear solving system, in addition to the rotorcraft balance force and moment balance equations of Eq. 1, the presence of the Lagrange multipliers also allows the introduction of additional arbitrary constraints in the problem statement, thus enabling the possibility of including bounds to critical design parameters like, for instance, flapping motion and aircraft attitude.

On the other hand, the Lagrangian multipliers used in energy-minimum problem cause an increase of the number of unknowns and, consequently, of the size of the nonlinear problem to be numerically solved, and of the corresponding computational cost. This drawback can be alleviated by using suitable solution strategies like, for instance, the application (when possible) of the multirotor transformation that allows the reduction of the number of control variables. However, the increase in computational costs is not an issue for all non real-time applications, like the off-line scheduling of the commands necessary to trim the vehicle for a given set of flight conditions.

The satisfaction of the constrained minimum-energy problem in Eq. 2 corresponds to the solution of the following system of equations

$$(3) \quad \begin{cases} \frac{\partial F}{\partial \mathbf{x}} = 0 \\ \frac{\partial F}{\partial \boldsymbol{\lambda}} = 0 \\ \frac{\partial F}{\partial \mathbf{u}} = 0 \end{cases}$$

Limiting the constraints to the aircraft balance equations, this system is composed of 5 equations given by $\partial F/\partial \mathbf{x} = 0$, n equations given by $\partial F/\partial \mathbf{u} = 0$ and 9 equations provided by $\partial F/\partial \boldsymbol{\lambda} = 0$ (namely, those Eq. 1), with the $5 + n + 9$ unknowns, $(\mathbf{x}, \mathbf{u}, \boldsymbol{\lambda})$.

Thus, Eqs. (3) yield a consistent nonlinear system that can be appropriately solved through the standard Newton-Raphson method. Since its solution through the Newton-Raphson method requires the evaluation of the Hessian matrix of F, a not negligible computational effort in evaluating its second derivatives could represent a numerical issue (although the Hessian matrix is symmetric). To alleviate this critical point, the application of the SLSQP algorithm suitable for non-linear constrained minimization problems is also examined [15].

Finally, note that this approach can also be applied for the standard trim problem with 4. Indeed, in this case the energy problem corresponds to a 18-equation system with 18 unknowns, providing the trim conditions that minimize the defined energy function.

2.2. Trim solver description

The trim solver is obtained, for a given set of kinematic variables, **x**, and commands, **u**, by combining the aerodynamic/propulsive loads (X, Y, Z, L, M, N) produced by each vehicle component with the gravitational and inertial loads. The aerodynamic interaction effects between components are either neglected or modeled through semi-empirical coefficients[16].

For each rotor, the aeroelastic response to four commands (namely, angular speed Ω, collective pitch θ_0, lateral pitch θ_c and longitudinal pitch θ_c) and to the hub kinematics (given in terms of u, v, w, p, q, r) is evaluated. The rotor blade is modelled as hinged, rigid structure, with lead-lag and flap motion in addition to rotation about the feathering axis. The aerodynamic loads are determined by a quasi steady Blade Element Momentum Theory, where the section aerodynamic lift, drag and pitch moment are evaluated through a lookup table approach. The three-dimensional effects are included through wake inflow models, along with the Prandtl root and tip losses function [10].

The blade dynamics equations are solved through a harmonic balance technique, from which the steady loads at the rotor hub are obtained as a combination of the zero-th and first harmonics of the blade root loads in the rotating frame [17]).

The aerodynamic fuselage loads are evaluated through aerodynamic coefficients defined in the wind frame of reference using the Flat Plate Area method.

The solution of the trim problem is obtained through two nested iterative loops, one for the solution of Eqs. (3) and the other for the solution of the rotor dynamics equations. Specifically, starting from current states, $(\mathbf{x}, \mathbf{u})$, the aerodynamic loads of each rotorcraft component are evaluated, with inclusion of those from rotors given as output of the harmonic balance problem and then, these are used to define a new value of the functions in Eq. 3, and hence determine a new value of the unknowns to be applied in the next step of the trim loop. This procedure is iterated until convergence.

3. NUMERICAL RESULTS

The numerical investigation herein proposed regards both a quadcopter and a hexacopter configuration. For both of them, the control energy is assumed to be the energy function to be minimised (unless expressly stated otherwise), and the control strategies investigated are:

- Strategy A, pure blade collective pitch control;
- Strategy B, pure rotor angular velocity control;
- Strategy C, combined angular velocity and blade collective pitch control.

The proposed approach is validated against numerical results available in the literature for the control strategies A and B applied to a quadcopter [18] (no complete literature data are available for the hexacopter configuration).

3.1. Quadcopter

The main characteristics of the quadrotor configuration are given in Tab. 1, whereas its schematic representation is shown in Fig. 1.

For the free stream velocity ranging from $V = 0$ kts to $V = 90$ kt, Fig. 2 and Fig. 3 present

Table 1: Quadcopter characteristics.

Maximum take-off weight =	3000 kg
Radius, R =	4.0081 m
Blade counts, N_b =	3
Root cut-off, R_{c_0} =	0.1 R
Mean chord, c_m =	0.2711 m
Linear twist =	12°
Taper ratio =	1
Solidity, σ =	0.0646
Airfoil =	VR7

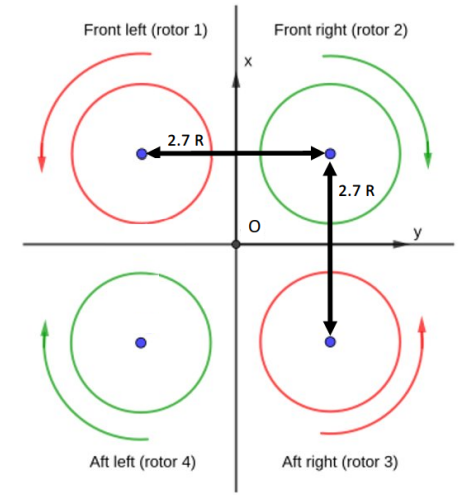

(a) top view

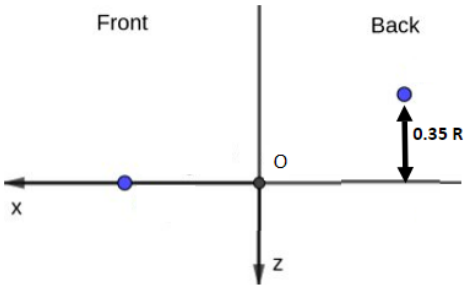

(b) lateral view

Figure 1: Schematic representation of the quadcopter configuration.

the comparison with the literature results given, respectively, in terms of control settings (blade pitch, $\theta_{75\%}$, for strategy A, and angular velocity, Ω, for strategy B) and trim rotor loads. The rotor loads are expressed as the ratio between the thrust coefficient, c_T, and the rotor solidity, σ, and as the dimensionless mean hub moment, $M_{hm} = \sqrt{M_x^2 + M_y^2}/(TR)$, with M_x, M_y and T denoting the rolling and pitching moments, and rotor thrust. Following [18], when the control variable corresponds to the angular velocity, the blade pitch is set to $\theta_{75\%} = 7°$, whereas when the collective pitch is the control variable the rotor angular velocity is set equal to $327 rpm$.

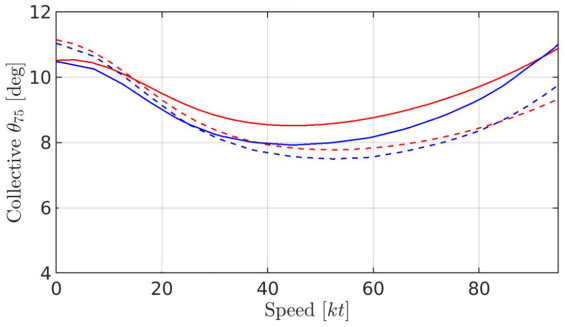

(a) Strategy A

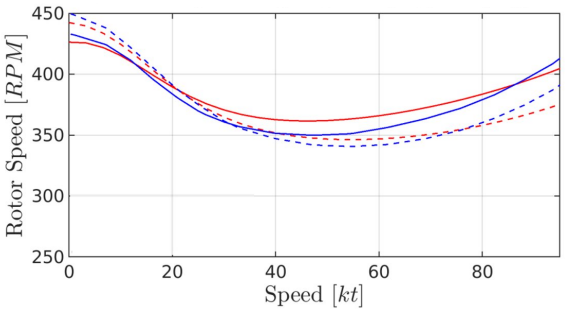

(b) Strategy B

Figure 2: Comparison between predicted control settings (red lines) and results of Shastry et al.[18] (blue lines). Solid lines represent front rotors loads, dashed lines represent aft rotor loads.

Fig. 2 shows that the collective angles (strategy A) and the angular velocities (strategy B) of front and aft rotors present a similar trend as the freestream velocity increases: close to hovering condition both the collective angles and the angular velocities of the aft rotors are greater than those of the rear rotors, whereas the opposite occurs as the advancing velocity increases (aft and rear rotors curves intersect at advancing velocity equal to $V = 17$ kts for strategy A, and at advancing velocity equal to $V = 20$ kts for strategy B).

The comparisons between the hub loads (thrust and mean hub moment) given by the developed solver and those presented by Shastry et al.[18] are shown in Fig. 3. Similarly to the comparisons between the control settings provided in Fig. 2, the two predictions are in a quite satisfactory agreement. For both control settings and hub loads the overall trend is well captured, with some small discrepancies probably due to the different inflow models applied in the two approaches (no information is available about the inflow model used to obtain the literature results).

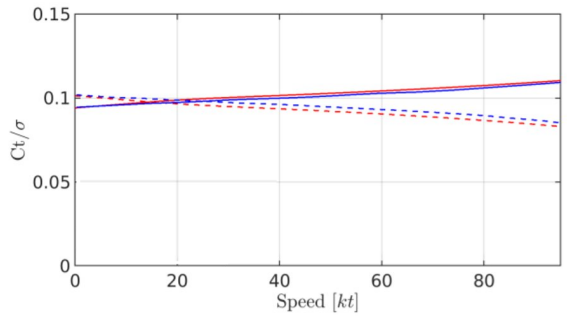

(a) Strategy A

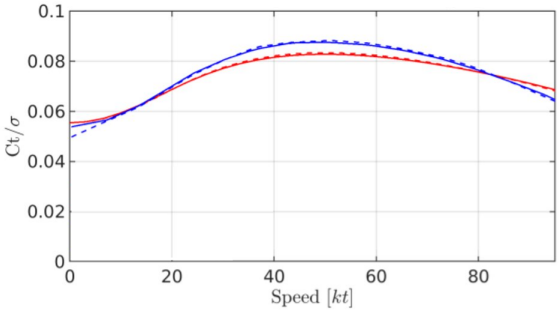

(b) Strategy B

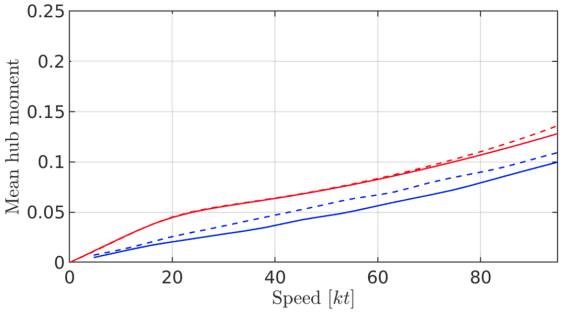

(c) Strategy A

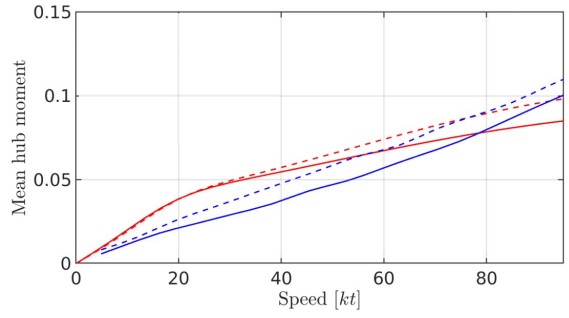

(d) Strategy B

Figure 3: Comparison between predicted rotor loads (red lines) and results of Shastry et al.[18] (blue lines). Solid lines represent front rotors loads, dashed lines represent aft rotor loads.

To get a better insight on the influence of the applied inflow model on the predictions, these are repeated by replacing the Pitt-Peters inflow model used to determine the results in Fig. 2 and Fig. 3 with the Glauert model. A 1% difference between the control settings solutions given by the two inflow models is observed.

Once validated, the proposed approach is applied with application of strategy C (in this case, comparisons with literature results are not available). In this case, the number of selected commands is equal to 8, and thus the use of the proposed methodology is a suitable, more general alternative to the application of the pseudo-inverse method. To speed up the numerical convergence of the solution algorithm, the commands are related to reference values (16° for the collective pitch and 30 rad/s for the angular velocity).

Figure 4 shows the comparison between the pitch settings obtained by the application of the three different strategies as the free-stream velocity increases. This comparison reveals that

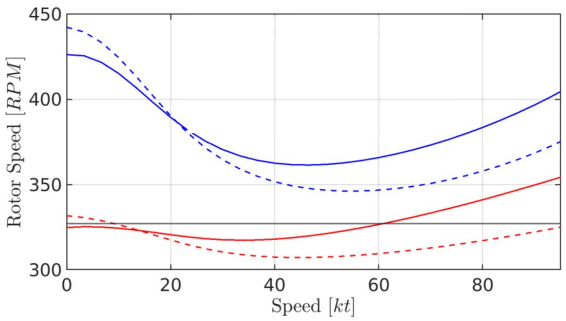

(a) rpm

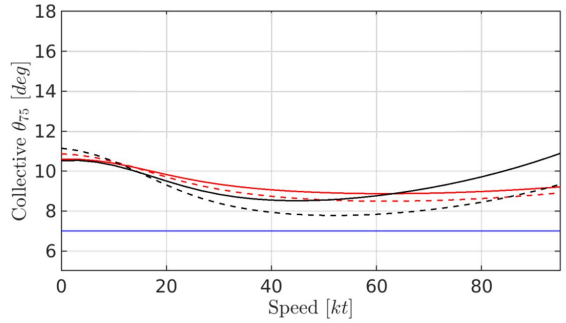

(b) collective pitch

Figure 4: Control settings obtained by the different trim strategies: strategy A (black lines); strategy B (blue lines); strategy C (red lines). Solid lines represent front rotors, dashed lines represent aft rotor.

the control strategies A and C provide similar values of both control settings, whereas strategy B requires a higher angular velocity (up to 100 rpm) than those requested by the other two strategies, due to the much lower value of the collective pitch angle. Instead, the observation of Fig. 5, which depicts comparisons among the

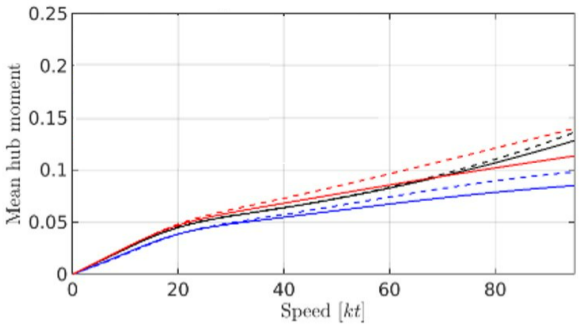

(a) Mean hub moment

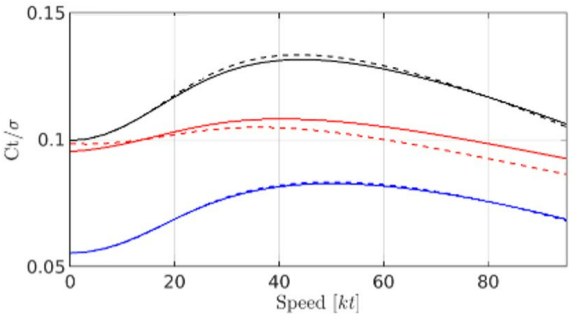

(b) Blade loading

Figure 5: Comparison between predicted rotor loads obtained by the different trim strategies: strategy C (red lines); strategy B (blue lines); strategy A (black lines). Solid lines represent front rotors, dashed lines represent aft rotors.

different strategies in terms of the corresponding rotor loads, reveals that the minimum blade loading and mean hub moment are achieved by application of strategy B (namely, when the required angular velocity is maximum).

3.2. Hexacopter

The hexacopter, schematically depicted in Fig. 6, has the same weight and geometric characteristics as the quadcopter (see Tab. 1), except for the rotor radius, which is equal to 3 m, and the solidity which is equal to $\sigma = 0.0863$. Unlike the quadrotor, all rotors are coplanar.

For this configuration, a more extensive investigation is performed to assess the robustness of the energy-based trim procedure, the effect of the root-finding algorithm (Newton-Raphson method or SLSQP algorithm) on accuracy and computational cost, and the influence of the control strategies and energy function definition on trimmed solution.

First, the trim procedure is applied with and without inclusion of wake inflow in rotor aerodynamic modelling. The motivation for this analysis is twofold: (i) to investigate the robustness of

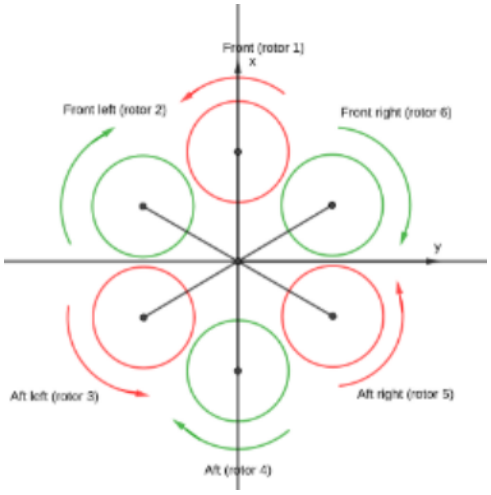

Figure 6: Schematic representation of the hexacopter configuration.

the procedure to the variation of the complexity of the problem, and (ii) to assess the effects of the wake inflow on the evaluation of the aerodynamic loads for non-conventional configurations (such as the hexacopter). It is performed for two flight velocities, $V = 0$ kts and $V = 50$ kt, using the Glauert inflow model (when present), and the Newton-Raphson algorithm as the root-finding method (the Jacobian is a $[20x20]$ square matrix).

For the hovering case and the control Strategy B, regardless of the inflow correction, the angular velocities are the same for all rotors: equal to $\Omega = 39.3$ rad/s when the inflow is neglected, and equal to $\Omega = 60$ rad/s when it is included. Instead, for $V = 50$ kt, the results are shown in Tab. 2 in terms of control settings.

Table 2: Strategy B: Control settings for $V = 50$ kt (with $\theta_{75\%} = 16°$) with and without inflow model.

	no inflow	Glauert
Pitch	4.13°	3.89°
Ω_1	38.63 rad/s	44.13 rad/s
Ω_2	40.06 rad/s	46.03 rad/s
Ω_3	42.54 rad/s	49.51 rad/s
Ω_4	44.37 rad/s	50.90 rad/s
Ω_5	42.61 rad/s	49.52 rad/s
Ω_6	39.98 rad/s	46.02 rad/s

In this case, due to the geometric symmetry, regardless of the inflow model the control settings of rotors #2 and #6 are practically the same, and the same equivalence occurs for rotors #3 and #5. Furthermore, rotor #4 is that with the highest angular velocity to guarantee

the necessary vehicle attitude. The comparison of the results obtained with and without rotor inflow shows a maximum percentage variation equal to 34%, with an increase of the required angular velocities for the inflow case, to counterbalance its effects. Finally, the rotorcraft pitch angle is slightly lower when the wake inflow model is included.

The same analysis is performed for Strategy A. For the hovering case, the collective angle, equal for all rotors, is $\theta_{75\%} = 13.32$ deg when the inflow model is neglected, and is $\theta_{75\%} = 18.12$ deg when it is included. For the advancing case with $V = 50$ kt, Tab. 3 shows the results in terms of collective angles.

Table 3: Strategy A: control settings for $V = 50$ kt (with $\Omega = 50 rad/s$) with and without inflow model.

	no inflow	Glauert
Pitch	3.6°	3.6
$\theta_{75\%_1}$	13.38 deg	14.78 deg
$\theta_{75\%_2}$	13.58 deg	15.11 deg
$\theta_{75\%_3}$	13.96 deg	15.78 deg
$\theta_{75\%_4}$	14.14 deg	16.08 deg
$\theta_{75\%_5}$	13.96 deg	15.79 deg
$\theta_{75\%_6}$	13.58 deg	15.10 deg

In this case, the maximum percentage variation due to the inflow is about 12%, with an increase of the collective angles in the inflow case to counterbalance its effects.

It is worth noting that, for all the analysed cases (for both strategies A and B), the inclusion of the inflow model strongly affects the computational costs that are almost doubled.

Furthermore, Fig. 7 shows the results in terms of control settings obtained by strategy C, for the forward velocity ranging from $V = 0$ kts to $V = 90$ kts, with inclusion of the Glauert wake-inflow model. Starting from coincident values of collective pitch and angular velocity of each rotor for the hovering condition, as the flight velocity increases the control settings of rotor #4 become higher than those of the other rotors, and the control settings of rotor #1 become lower. Furthermore, the differences between the angular velocities of the different rotors monotonically increase with the vehicle speed. Conversely, the differences in the collective angles of the rotors increase up to about $V = 50$ kts and then decrease. Note that, also in this case, due to the geometric symmetry of the configuration, the control settings of rotor #2 are equal to those of rotor #6 and the controls of rotor #3 are equal to

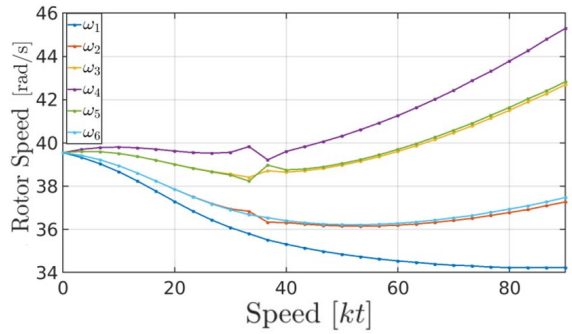

(a) rpm

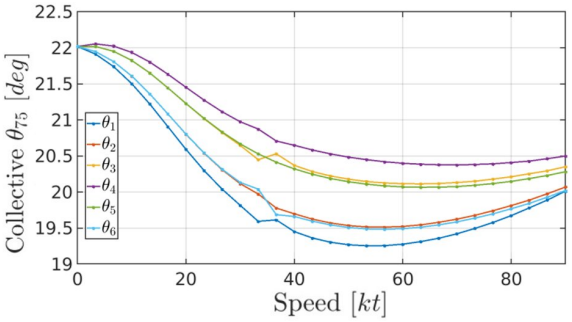

(b) collective

Figure 7: Strategy C: control settings

those of rotor #5, for all the tested velocities.

Due to the lack of complete literature data for the hexacopter configuration, the energy-based approach is indirectly validated for strategies A and B, through application of the multi-rotor transformation. Note that, in this case, the control variables of the energy-based method are equal to six, whereas they are reduced to four in the multirotor transform algorithm by eliminating the two redundant controls (namely, the second harmonic cyclic components). The analysis, not shown here for the sake of conciseness, prove that the two methodologies give similar results, with a maximum percentage error lower than 2%.

Next, the influence of the root-finding algorithms on solution accuracy and computational cost is analysed. To this aim, the trim of the aircraft with $V = 50$ kts is re-calculated by strategy C through the SLSQP algorithm. Tab. 4 depicts the comparison between each rotor trim angular velocity and collective angle given by the SQLQP results and those obtained through the Newton-Raphson method.

It shows an excellent level of agreement between the two predictions, with 0.3% averaged percentage difference for the angular velocities and 0.35% averaged percentage difference for the collective angles. Instead, the computa-

Table 4: Strategy C: control settings obtained for $V = 50$ kt. Trim procedure solved through Newton-Raphson (NR) and SLSQP algorithms.

	$\theta_{75\%}[deg]$		$\Omega[rad/s]$	
Rotor	NR	SLSQP	NR	SRSQP
#1	19.27	19.34	34.85	34.94
#2	19.53	19.51	36.16	36.18
#3	20.17	20.16	38.97	39.03
#4	20.48	20.44	40.32	40.16
#5	20.14	20.20	39.05	39.33
#6	19.50	19.38	36.22	36.02

tional cost is quite different, with the time required to minimize the cost function through the Newton-Raphson equal to 30 min, and that required by the SLSQP algorithm equal to 20 min, both running on a machine with 2xCPU Xeon E5-2660 v4 (14 physical cores, 28 logical cores) 128 GB RAM. Thus, at least for the analysed cases, the SLSQP method seems to outperform the Newton-Raphson one, although its convergence behaviour seems to be more sensitive to the assigned initial guess.

To reduce the computational costs of the solution method based on the Newton-Raphson algorithm while maintaining its good convergence characteristics, the multirotor transform is applied within the energy-based approach. Indeed, the multirotor technique allows the reduction of the number of unknowns (commands) of the problem, thus yielding a reduced-order energy-based method, with the consequent reduction of the dimension of the Jacobian matrix and of the computational costs). This procedure is particularly effective in problems with many control variables, for which the multirotor transform order reduction is significant.

This approach is tested on the hexacopter configuration for the trim strategy C, assuming the advancing velocity equal to $V = 50$ kt. First, the application of the multirotor transform provides a reduced problem composed of a set of eight primary controls (collective, cyclic, and differential controls for both angular velocity and collective pitch angle), that replaces the original set of twelve controls. Next, the Newton-Raphson algorithm is applied for the solution of the energy-based problem and then, the inverse multirotor transform [9] gives back the twelve controls to be actuated (see Tab. 5). The comparison of the results in Tab. 5 with those in Tab. 4 shows that the two methodologies provide similar results, with a maximum percentage difference of about 0.9% for collective angles and about 1.5% for angular velocities. Furthermore, the time required for the simulation is 21 min, in line with that of the SLSQP algorithm.

Table 5: Strategy C: control settings for $V = 50$ kts through the combined use of multirotor transform and energy-based trim.

Rotor	$\theta_{75\%}[deg]$	$\Omega[rad/s]$
#1	19.13	35.35
#2	19.45	36.12
#3	20.32	38.91
#4	20.52	39.94
#5	20.20	39.17
#6	19.34	36.38

Finally, the energy-based method is applied assuming the hub torque as the function to minimize. Tab. 6 presents the results in terms of control settings for trim strategy C and advancing velocity $V = 50$ kt.

Table 6: Strategy C: control settings for $V = 50$ kts torque minimization.

Rotor	$\theta_{75\%}[deg]$	$\Omega[rad/s]$
#1	16.93	40.75
#2	17.45	41.70
#3	18.41	42.79
#4	18.84	43.10
#5	18.41	42.79
#6	17.45	41.68

These results reveal slightly lower values of the collective angles compared to those provided by the control-energy-based problem and higher values of the angular velocities. These differences yield different aerodynamic loads, as shown in Tab. 7 and Tab. 8 that present the magnitude of the aerodynamic loads corresponding, respectively, to the control-energy-based and torque-based trim.

As expected, the torque of all rotors is lower when the torque-based trim is applied, with thrust higher for rotors #1, #2, and #6 (aft ones) and lower for rotors #3, #4, and #5 (rear ones). The H-force, the S-force, and the rolling and pitching moments are higher for all the rotors in the case of control-energy-based trim.

4. CONCLUSIONS

This paper presents a novel procedure to identify the trim conditions of multirotor configurations, in the presence of redundant (> 4) con-

Table 7: Strategy C: magnitude of aerodynamic loads for $V = 50$ kts and control-energy-based trim.

Rotor	#1	#2-#6	#3-#5	#4
H-force [N]	378	426	551	615
S-force [N]	140	147	160	164
Thrust [N]	3939	4348	5372	5905
M_x^a [Nm]	546	484	340	268
M_y^a [Nm]	2046	2150	2373	2468
Torque [Nm]	410	454	576	645

Table 8: Strategy C: magnitude of aerodynamic loads for $V = 50$ kts and torque-based trim.

Rotor	#1	#2-#6	#3-#5	#4
H-force [N]	295	348	450	499
S-force [N]	74	84	104	115
Thrust [N]	3994	4490	5332	5685
M_x^a [Nm]	159	124	83	72
M_y^a [Nm]	1708	1843	2079	2181
Torque [Nm]	390	437	522	559

trols. This procedure recasts the trim search into a constrained minimum energy problem, with the objective function suitably selected by the designer (actuation energy, performance, noise, vibrations, etc.), and the rotorcraft equilibrium equations included as constraints. The proposed trim approach is validated against data in the literature for a quadrotor configuration, and validated by comparison with the results from a standard multirotor strategy for a hexacopter configuration (no complete literature data are available, in this case). The numerical investigation on quadcopter and hexacopter configurations showed that:

- The level of complexity of the rotorcraft model does not affect the effectiveness of the proposed methodology. The examination of this issue, accomplished by including or not a wake inflow model in the evaluation of the aerodynamic loads of rotors, also provides the assessment of the wake inflow influence in non-conventional configurations (such as the hexacopter). As expected, akin to conventional rotorcraft, the use of an inflow model is fundamental to get a reliable estimation of aerodynamic loads and, in turn, of control settings for non-conventional configurations (for the cases analysed in this work, underestimation of the control settings of about 30% is achieved without wake inflow effects). Furthermore, the type of inflow model used only slightly affects the solution (differences of control setting are lower than 1% , for the analysed cases).

- The accuracy of the root-finding algorithms used to solve the constrained minimization problem (Newton-Raphson and SLSQP) is comparable, with a difference in terms of average relative error lower than 1%. The SLSQP algorithm has better computational efficiency than the Newton-Raphson algorithm, similar to that achievable by introducing a standard multirotor transform method. However, the SLQLP presents convergence issues related to the assignment of the initial guess, which seem to be significantly alleviated when the Newton-Raphson method is used. Hence, a trim tool requiring limited computational cost and having good convergence properties is defined by the combination of the multirotor transform and the energy-based approach, with the Newton-Raphson method used for the root-finding procedure. This approach is proven to be effective, giving results similar to those from Newton-Raphson and SLSQP algorithms applied without multirotor transformation (percentage differences of about 1% for collective angles and about 1.5% for angular velocities are achieved), while reducing the computational time with respect to the SLSQP algorithm.

- The application of the proposed method to different objective functions shows its potentiality in exploiting redundant controls to optimize rotorcraft features (like emitted noise, performance, vibrations, etc.) through the definition of suitable configurations in the vehicle trim process.

REFERENCES

[1] Nicholas Polaczyk, Enzo Trombino, Peng Wei, and Mihaela Mitici. A review of current technology and research in urban on-demand air mobility applications. In *8th Biennial Autonomous VTOL Technical Meeting and 6th Annual Electric VTOL Symposium*, Mesa, AZ, 2019.

[2] Christopher Silva, Wayne R Johnson, Eduardo Solis, Michael D Patterson, and Kevin R Antcliff. VTOL urban air mobility concept vehicles for technology development. In *2018 Aviation Technology, Inte-*

gration, and Operations Conference, Atlanta, Georgia, 2018.

[3] eVTOL news. https://evtol.news/aircraft, 2022.

[4] Pipistrel Alpha Electro. https://www.pipistrel-usa.com/alpha-electro, Accessed 27 January 2022.

[5] Aurora Flight Sciences Pegasus PAV. https://evtol.news/aurora/, Accessed 5 February 2022.

[6] Lilium jet. https://evtol.news/lilium/, Accessed 5 February 2022.

[7] Caterina Poggi, Monica Rossetti, Giovanni Bernardini, Umberto Iemma, Cristiano Andolfi, Christian Milano, and Massimo Gennaretti. Surrogate models for predicting noise emission and aerodynamic performance of propellers. *Aerospace Science and Technology*, 125:107016, 2022.

[8] Michael E McKay, Robert Niemiec, and Farhan Gandhi. Analysis of classical and alternate hexacopter configurations with single rotor failure. *Journal of Aircraft*, 55(6):2372–2379, 2018.

[9] Robert Niemiec and Farhan Gandhi. Multirotor coordinate transforms for orthogonal primary and redundant control modes for regular hexacopters and octocopters. In *42nd Annual European Rotorcraft Forum*, Lille, France, 2016.

[10] Wayne Johnson. *Rotorcraft aeromechanics*, volume 36. Cambridge University Press, 2013.

[11] Caterina Poggi, Giovanni Bernardini, and Massimo Gennaretti. Influence of trim control strategy on noise radiated by multirotor systems. In *28th AIAA/CEAS Aeroacoustics 2022 Conference*, page 2971, 2022.

[12] Bernard Etkin and Lloyd Duff Reid. *Dynamics of flight: stability and control*. Wiley, New York; Brisbane, 3rd ed. edition, 1996.

[13] Tjalling J Ypma. Historical development of the newton–raphson method. *SIAM review*, 37(4):531–551, 1995.

[14] Francis Begnaud Hildebrand. *Introduction to numerical analysis*. McGraw-Hill New York, 1956.

[15] D. Kraft. *A Software Package for Sequential Quadratic Programming*. Deutsche Forschungs- und Versuchsanstalt für Luft- und Raumfahrt Köln: Forschungsbericht. Wiss. Berichtswesen d. DFVLR, 1988.

[16] Daniel Raymer. *Aircraft design: a conceptual approach*. American Institute of Aeronautics and Astronautics, Inc., 2012.

[17] Richard L Bielawa. *Rotary wing structural dynamics and aeroelasticity*. American Institute of Aeronautics and Astronautics, 2006.

[18] Abhishek Shastry and Anubhav Datta. Predicting wake and structural loads in RPM controlled multirotor aircraft. In *Vertical Flight Society's Transformative Vertical Flight 2020 Technical Meeting*, San Jose, CA, 2020.